Generating function of the tilings of Aztec rectangle with holes

Tri Lai[*]

Institute for Mathematics and its Applications

Minneapolis, MN 55455

`tmlai@ima.umn.edu`

Abstract

We consider a generating function of the domino tilings of an Aztec rectangle with several boundary unit squares removed. Our generating function involves two statistics: the rank of the tiling and half number of vertical dominoes as in the Aztec diamond theorem by Elkies, Kuperberg, Larsen and Propp. In addition, our work deduces a combinatorial explanation for an interesting connection between the number of lozenge tilings of a semihexagon and the number of domino tilings of an Aztec rectangle.

Keywords: perfect matchings, tilings, dual graph, Aztec diamonds, Aztec rectangles.

1 Introduction

A lattice partitions the plane into fundamental regions. A (lattice) *region* considered in this paper is a finite connected union of fundamental regions. A *tile* is the union of any two fundamental regions sharing an edge. A *tiling* of a region is a covering of the region by tiles so that there are no gaps or overlaps.

The *Aztec diamond* of order n is the union of all unit squares inside the contour $|x|+|y| = n+1$ (see Figure 1.1 for several first Aztec diamonds). For each (domino) tiling T of the Aztec diamond, we denote by $v(T)$ haft number of vertical dominoes in T, and $r(T)$ the *rank* of T that is defined as follows. The *minimal tiling* T_0 consisting of all horizontal dominoes has rank 0; and the rank $r(T)$ of T is the minimal number of *elementary moves* required to reach T from T_0 (see Figure 1.2(a) for two types of the elementary moves, and Figures 1.2(b)–(e) for several domino tilings of the Aztec diamond of order 2 together with their ranks).

Elkies, Kuperberg, Larsen and Propp [4] proved a simple product formula for the generating function of the tilings of an Aztec diamond.

Theorem 1.1 (Aztec Diamond Theorem [4])**.** *For positive integer n*

$$\sum_{T} q^{r(T)} t^{v(T)} = \prod_{k=0}^{n-1} (1 + tq^{2k+1})^{n-k}, \tag{1.1}$$

where the sum is taken over all tilings T of the Aztec diamond region of order n.
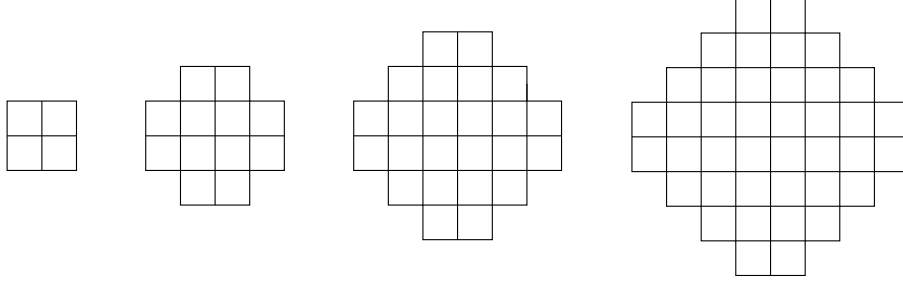
Figure 1.1: From left to right, the Aztec diamonds of order 1, 2, 3 and 4.

(a)
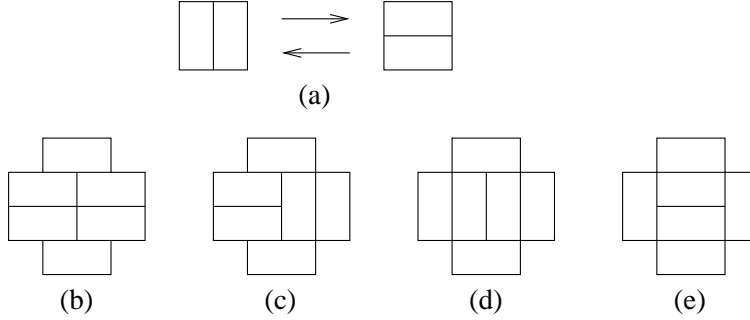

(b)   (c)   (d)   (e)

Figure 1.2: (a) The elementary moves: rotations of a 2×2 block of two vertical or horizontal dominoes. (b) The minimal tiling of the Aztec diamond of order 2. (c) A tiling of rank 1. (d) A tiling of rank 2. (e) A tiling of rank 3.

The $t = q = 1$ specialization of the Aztec Diamond Theorem implies that the number of tilings of the Aztec diamond of order n is equal to $2^{n(n+1)/2}$. Besides the fours original proofs in [4], a number of further proofs of the Aztec Diamond Theorem and its special cases have been given by several authors (see e.g. [1], [2], [5], [7], [8], [11]). Moreover, we proved in [10] a generalization of the above unweighted Aztec Diamond Theorem for a family of 4-vertex regions on the square lattice with diagonals drawn in.

The Aztec rectangle is a natural generalization of the Aztec diamond. Figure 1.3(a) shows an example of the Aztec rectangle. Denote by $\mathcal{AR}_{m,n}$ the Aztec rectangle having m unit squares on the southwest side and n unit squares along the northwest side. For $m < n$, $\mathcal{AR}_{m,n}$ does not have any tiling, however when we remove $n - m$ unit squares along the southeast side, the number of tilings of the resulting region is given by a simple product formula (see e.g. [6], Lemma 3). Denote by $\mathcal{AR}_{m,n}(s_1, s_2, \ldots, s_m)$ the $(m \times n)$-Aztec rectangle, where all unit squares on the southeast side, except for the s_1-st, the s_2-nd, $\ldots$ and the s_m-th ones, have been removed (see Figure 1.3(b) for an example). We call the unit squares, which have been removed, *holes*, and our region an *Aztec rectangle with holes*.

In general, an Aztec rectangle with holes does not admit a tiling consisting of all horizontal dominoes. Assume that $\{h_1, \ldots, h_{n-m}\}$ $(= \{1, 2, \ldots, n\} - \{s_1, \ldots, s_m\})$ is the position set of the holes. We (re-)define our minimal tiling (still denoted by T_0) as follows: Next to the hole at the position h_i on the southeast side, we place southeast-to-northwest strip of $m - (h_i - i)$ vertical dominoes, for $i = 1, 2, \ldots, n-m$, and cover the rest of the region by horizontal dominoes. Figure 1.3(c) illustrates the minimal tiling of the region $\mathcal{AR}_{3,6}(1, 4, 6)$. We define two statistics r and
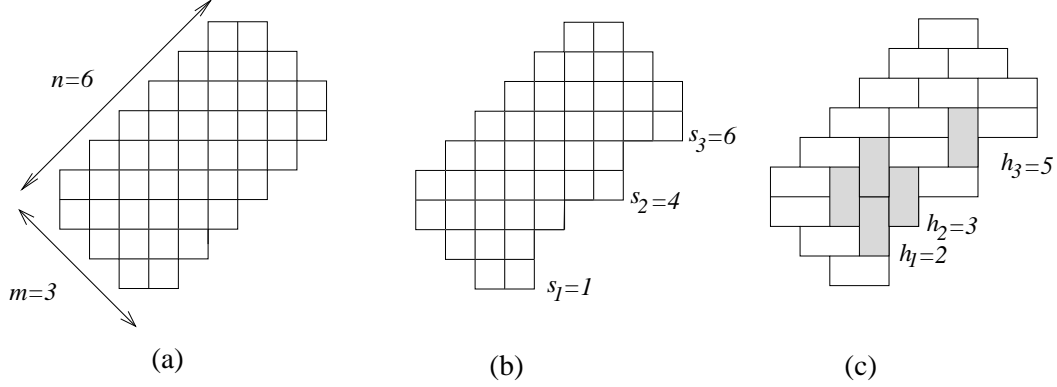
2

Figure 1.3: (a) The Aztec rectangle $\mathcal{AR}_{3,6}$. (b) The Aztec rectangle with holes $\mathcal{AR}_{3,6}(1,4,6)$. (c) The minimal tiling of $\mathcal{AR}_{3,6}(1,4,6)$.

v for an Aztec rectangle with holes in the same way as the case of the Aztec diamonds.

We consider the following tiling generating function

$$F(q,t) := \sum_T q^{r(T)} t^{v(T)}, \tag{1.2}$$

where the sum is taken over all tilings T of $\mathcal{AR}_{m,n}(s_1, s_2, \ldots, s_m)$. The main result of our paper is the following theorem.

Theorem 1.2. *Assume $m, n, s_1, s_2, \ldots, s_m$ are positive integers, so that $m < n$ and $1 \leqslant s_1 < s_2 < \ldots < s_m \leqslant n$. Then the tiling generating function of $\mathcal{AR}_{m,n}(s_1, s_2, \ldots, s_m)$ is given by*

$$F(q,t) = q^{\frac{2(m-1)m(m+1)}{3} + 2\sum_{i=1}^{m}(s_i - i) - \sum_{1 \leqslant i \leqslant j \leqslant m} 2(s_i + j - i - 1)} \tag{1.3}$$

$$\times \prod_{k=0}^{m-1} (1 + tq^{2k+1})^{m-k} \prod_{1 \leqslant i < j \leqslant m} \frac{q^{2s_j} - q^{2s_i}}{q^{2j} - q^{2i}}. \tag{1.4}$$

2   Subgraph replacements

The *dual graph* of a region R is the graph whose vertices are the fundamental regions of R and whose edges connect precisely two fundamental regions sharing an edge. A *perfect matching* of a graph G is a collection of disjoint edges covering all vertices of G. The tilings of a region can be identified naturally with the perfect matchings of its dual graph.

Let G be a weighted graph. The *matching generating function* $M(G)$ of G is defined to be the sum of weights of all perfect matchings of G, where the *weight* of a perfect matching is the product of weights of its constituent edges. If the tiles of a region R carry some weights, we define similarly the *tiling generating function* $M(R)$ of the region R. Moreover, each edge of the dual graph G of the region R carries the same weight as its corresponding tile in R.

Next, we present several preliminary results of the subgraph replacement method.

Lemma 2.1 (Vertex-Splitting Lemma). *Let G be a weighted graph and v a vertex of G. Denote by $N(v)$ the set vertices adjacent to v. For any disjoint union $N(v) = H \cup K$, let G' be the*
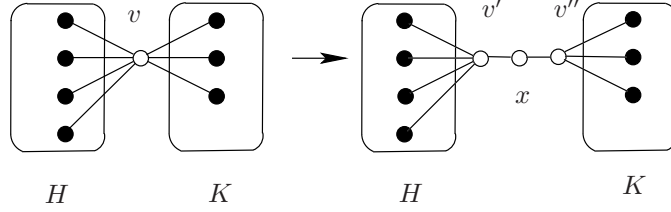
3

Figure 2.1: Vertex splitting.
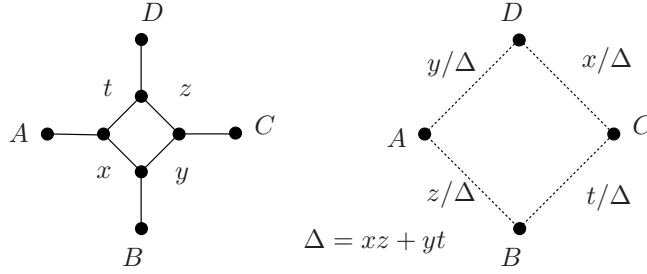

$$\Delta = xz + yt$$

Figure 2.2: Urban renewal.

graph obtained from $G \setminus v$ by including three new vertices v', v'' and x so that $N(v') = H \cup \{x\}$, $N(v'') = K \cup \{x\}$, and $N(x) = \{v', v''\}$ (see Figure 2.1). Then $\mathrm{M}(G) = \mathrm{M}(G')$.

Lemma 2.2 (Star Lemma)**.** *Let G be a weighted graph, and let v be a vertex of G. Let G' be the graph obtained from G by multiplying the weights of all edges incident to v by $t > 0$. Then $\mathrm{M}(G') = t\,\mathrm{M}(G)$.*

The following result is a generalization (due to Propp) of the "urban renewal" trick first observed by Kuperberg.

Lemma 2.3 (Spider Lemma)**.** *Let G be a weighted graph containing the subgraph K shown on the left in Figure 2.2 (the labels indicate weights, unlabeled edges have weight 1). Suppose in addition that the four inner black vertices in the subgraph K, different from A, B, C, D, have no neighbors outside K. Let G' be the graph obtained from G by replacing K by the graph $\overline{K}$ shown on right in Figure 2.2, where the dashed lines indicate new edges, weighted as shown. Then $\mathrm{M}(G) = (xz + yt)\,\mathrm{M}(G')$.*

A *forced edge* of a graph G is an edge contained in every perfect matching of G. Assume that G is a weighted graph with weight assignment wt on its edges, and G' is obtained from G by removing forced edges $e_1, \ldots, e_k$, and removing the vertices incident to those edges. Then one clearly has

$$\mathrm{M}(G) = \mathrm{M}(G') \prod_{i=1}^{k} \mathrm{wt}(e_i).$$

Hereafter, whenever we remove some forced edges, we remove also the vertices incident to them.

Denote by $AR_{m,n}$ the dual graph of the Aztec rectangle $\mathcal{AR}_{m,n}$ rotated 45^0 clockwise. The graph $AR_{m,n}$ consists of m rows and n columns of 4-cycles (see shaded diamonds in Figure 2.3(a)). We call this graph an *Aztec rectangle graph*. If one removes all bottommost vertices of
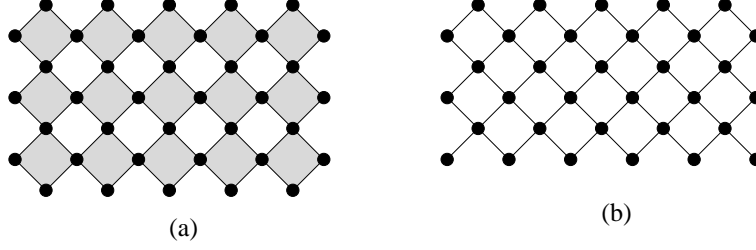
4

Figure 2.3: (a) The Aztec rectangle graph $AR_{3,5}$ with diamond-faces shaded. (b) The baseless Aztec rectangle graph $AR_{3-\frac{1}{2},5}$.
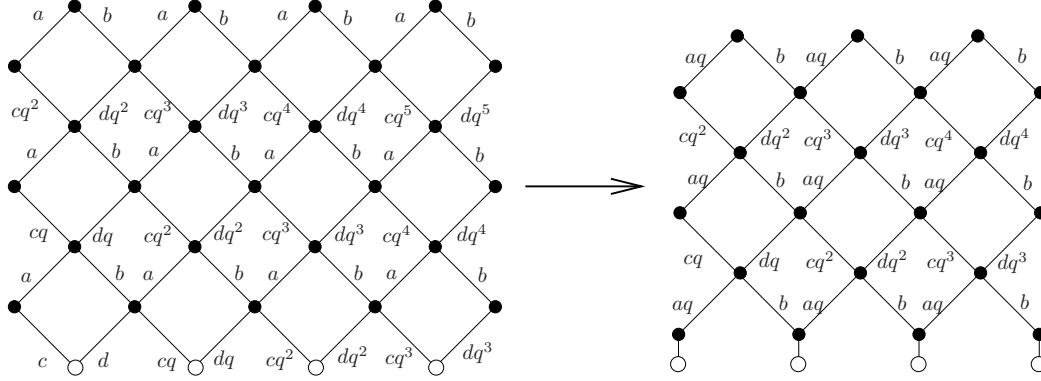

Figure 2.4: Illustrating the replacement rule in Lemma 2.4. The white circles indicate the vertices $v_1, v_2, \ldots, v_n$.

$AR_{m,n}$, the resulting graph is denoted by $AR_{m-\frac{1}{2},n}$, and called a *baseless Aztec rectangle graph* (see Figure 2.3(b) for an example).

Assume a, b, c, d, q are positive numbers. We consider the weight assignment $\mathrm{wt}_{c,d}^{a,b}(q)$ on the edges of $AR_{m,n}$ as follows. The diamond-face on row i (from bottom to top) and column j (from left to right) have edge-weights $a, b, dq^{i+j-2}, cq^{i+j-2}$ (in clockwise order, starting from the northwest edge). See the left picture in Figure 2.4 for the case $m = 3$ and $n = 4$. Denote by $AR_{m,n}\left(\mathrm{wt}_{c,d}^{a,b}(q)\right)$ the resulting weighted Aztec rectangle graph; and, similar to the unweighted case, denote by $AR_{m-\frac{1}{2},n}\left(\mathrm{wt}_{c,d}^{a,b}(q)\right)$ the weighted baseless Aztec rectangle graph obtained from $AR_{m,n}\left(\mathrm{wt}_{c,d}^{a,b}(q)\right)$ by removing the bottommost vertices.

The *connected sum* $G\#G'$ of two disjoint graphs G and G' along the ordered sets of vertices $\{v_1, \ldots, v_n\} \subset V(G)$ and $\{v_1', \ldots, v_n'\} \subset V(G')$ is the graph obtained from G and G' by identifying vertices v_i and v_i', for $i = 1, \ldots, n$.

Lemma 2.4. *Let G be a graph and let $\{v_1, \ldots, v_n\}$ be an ordered subset of its vertices. Then*

$$\mathrm{M}\left(AR_{m,n}\left(\mathrm{wt}_{c,d}^{a,b}(q)\right)\#G\right) = (ad+bc)^m q^{\frac{m(m-1)}{2}} \mathrm{M}\left({}_{|}AR_{m-\frac{1}{2},n-1}\left(\mathrm{wt}_{c,d}^{aq,b}(q)\right)\#G\right), \quad (2.1)$$

where ${}_{|}AR_{m-\frac{1}{2},n-1}\left(\mathrm{wt}_{c,d}^{a,b}(q)\right)$ *is obtained from the graph* $AR_{m-\frac{1}{2},n-1}\left(\mathrm{wt}_{c,d}^{a,b}(q)\right)$ *by appending*
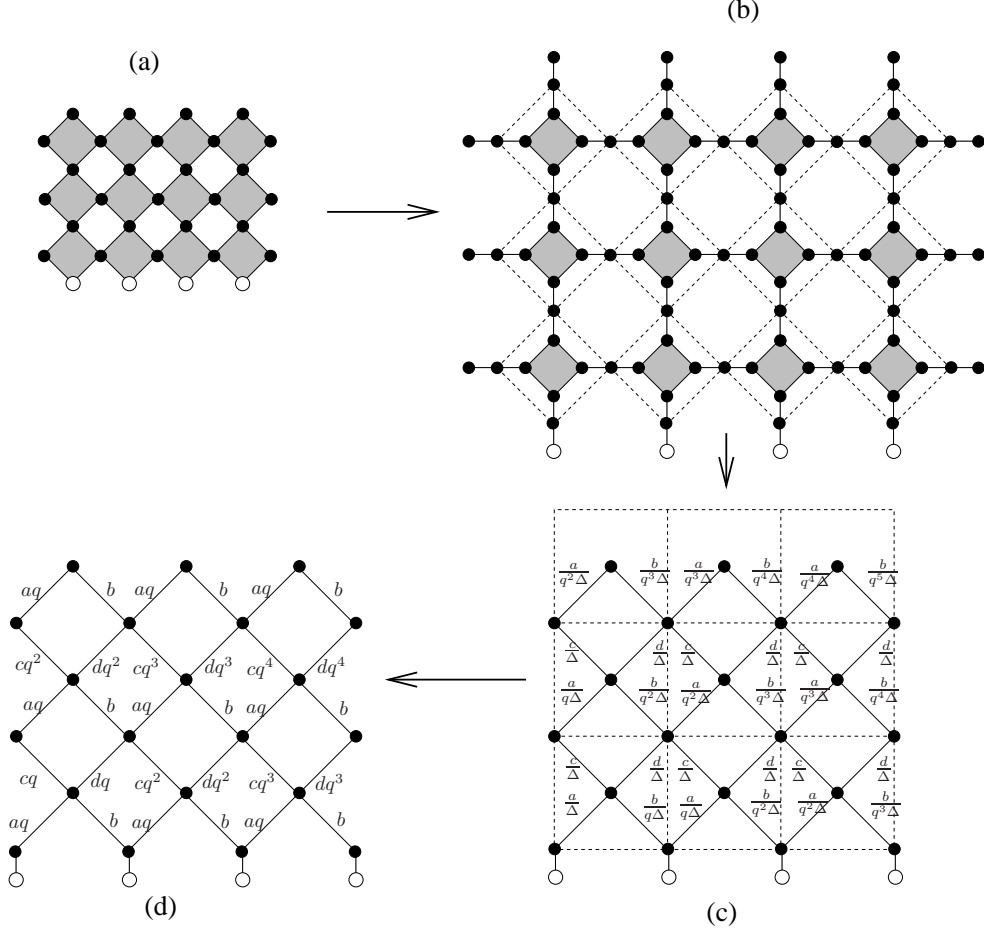
Figure 2.5: Illustrating the proof of Lemma 2.4.

vertical edges from their bottommost vertices; and where the connected sum acts on G along $\{v_1, \ldots, v_n\}$, and on other summands along their bottommost vertices (ordered from left to right).

The replacement in Lemma 2.4 is illustrated in Figure 2.4 for $m = 3$ and $n = 4$. We note that the unweighted version (when $a = b = c = d = q = 1$) of Lemma 2.4 was introduced in [9] (see Lemma 3.5).

Proof. The proof is based on Figure 2.5, for $m = 3$ and $n = 4$. First, we apply Vertex-Splitting Lemma 2.1 to vertices of $_|AR_{m,n}\left(\text{wt}_{c,d}^{a,b}(q)\right)$ in the graph on the left-hand side of (2.1) as in Figures 2.5(a) and (b); the sides of the shaded diamonds are weighted as in the left picture in Figure 2.4. Denote by G_1 the resulting graph.

Next, we apply Spider Lemma 2.3 around all shaded diamonds in G_1, and remove all m leftmost horizontal edges, m rightmost horizontal edges and n topmost vertical edges, which are forced (see Figure 2.5(b)). We get the graph $G_2 = AR_{m-\frac{1}{2},n-1}(\text{wt}')\#G$, where $AR_{m-\frac{1}{2},n-1}(\text{wt}')$ is a weighted version of $AR_{m-\frac{1}{2},n-1}$ with edges weighted as in Figure 2.5(c), and where $\Delta = ad + bc$.

Finally, we use Star Lemma 2.2 to change the edge-weights in the graph G_2. Divide the graph $AR_{m-\frac{1}{2},n-1}(\text{wt}')$, except for vertical edges, into $m(n-1)$ subgraphs restricted by dotted

6

squares in Figure 2.5(c). Apply the Star Lemma with factor $q^{i+j-1}\Delta$ to the central vertex of the dotted square in row i and column j, for $i = 1, 2, \ldots, m$ and $j = 1, 2, \ldots, n-1$. This way, we obtain the graph on the right-hand side of (2.1).

By Vertex-Splitting, Spider and Star Lemmas, we get

$$\mathrm{M}\left({}_|AR_{m,n}\left(\mathrm{wt}_{c,d}^{a,b}(q)\right) \# G\right) = \mathrm{M}(G_1) \tag{2.2}$$

$$= \mathrm{M}(G_2) \prod_{1 \leqslant i,j \leqslant n} (q^{i+j-2}\Delta) \tag{2.3}$$

$$= \mathrm{M}\left(AR_{m-\frac{1}{2},n-1}(\mathrm{wt}_{c,d}^{aq,b}(q))\right) \prod_{1 \leqslant i \leqslant m, 1 \leqslant j \leqslant n-1} \left(q^{i+j-1}\Delta\right)^{-1} \prod_{1 \leqslant i,j \leqslant n} \left(q^{i+j-2}\Delta\right), \tag{2.4}$$

which implies (2.1). $\qquad\square$

3 Matching generating function of weighted Aztec rectangle graphs

In this section, we give an explicit formula for the matching generating function of the graph $AR_{m,n}\left(\mathrm{wt}_{c,d}^{a,b}(q)\right)$, where $m - n$ vertices on the base have been removed.

Given $\lambda_1 \geqslant \lambda_2 \geqslant \ldots \lambda_k \geqslant 0$, a *plane partition* of shape $(\lambda_1, \lambda_2, \ldots, \lambda_k)$ is an array of non-negative integers of the form

$$
\begin{array}{cccccc}
n_{1,1} & n_{1,2} & n_{1,3} & \ldots & \ldots & \ldots & n_{1,\lambda_1} \\
n_{2,1} & n_{2,2} & n_{2,3} & \ldots & \ldots & n_{2,\lambda_2} \\
\vdots & \vdots & \vdots & \vdots & \vdots & \\
n_{k,1} & n_{k,2} & n_{k,3} & \ldots & n_{k,\lambda_k}
\end{array}
\quad,
$$

where the entries are weakly decreasing across the rows and down the columns. A *column-strict plane partition* is a plane partition having entries in each column strictly decreasing. We refer reader to [12] for properties of column-strict plane partitions.

A *semihexagon* $\mathcal{SH}_{a,b}$ is the upper half of the semi-regular hexagon of side-lengths a, b, b, a, b, b (in clockwise order, starting from the northwest side) on the triangular lattice. We are interested in the (lozenge) tilings of the semihexagon $\mathcal{SH}_{a,b}$ with a up-pointing unit triangles removed from the base, which are called *dents*. Assume that the positions of the dents are $1 \leqslant s_1 < s_2 < \ldots < s_a \leqslant a + b$, we denote by $\mathcal{SH}_{a,b}(s_1, \ldots, s_a)$ the semihexagon with dents (see Figure 3.1 for an example; the black unit triangles indicate the dents).

Theorem 3.1. *Assume that m and n are two positive integers, so that $m < n$. The matching generating function of the weighted Aztec rectangle graph $AR_{m,n}\left(\mathrm{wt}_{c,d}^{a,b}(q)\right)$, where all bottom-most vertices, except for the s_1-st, the s_2-nd, $\ldots$ and the s_m-th ones, have been removed, equals*

$$q^{\frac{(m-1)m(m+1)}{3}+\sum_{i=1}^{m}(s_i-i)} a^{\sum_{i=1}^{m}(s_i-i)} b^{m(n-m)-\sum_{i=1}^{m}(s_i-i)} \prod_{k=1}^{m} \Delta_k^{m-k+1} \cdot \prod_{1 \leqslant i < j \leqslant m} \frac{q^{s_j} - q^{s_i}}{q^j - q^i}, \tag{3.1}$$
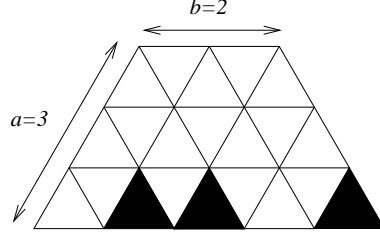
where $\Delta_k = adq^{k-1} + bc$.

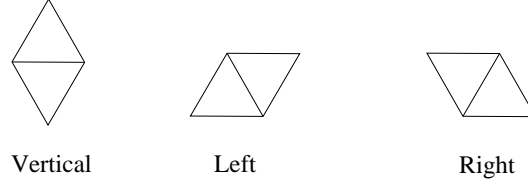Figure 3.1: The semihexagon with dents $\mathcal{SH}_{3,2}(2,3,5)$.

Figure 3.2: Three types of rhombi.

Proof. Denote by G our Aztec rectangle graph with $n-m$ bottommost vertices removed. Consider the graph G' obtained from $AR_{m,n}\left(\mathrm{wt}_{c,d}^{a,b}(t,q)\right)$ by adding a vertical edge (with weight 1) at all bottommost vertices, except for the ones at the positions s_i's (see Figure 3.3(a), for $m = 3$, $n = 5$, $s_1 = 2$, $s_2 = 3$, $s_3 = 5$). Then by considering forced edges, we get $\mathrm{M}(G) = \mathrm{M}(G')$.

Next, we apply a m-step transforming process based on Figure 3.3 as follows. First, apply the replacement rule in Lemma 2.4 as in Figures 3.3(a) and (b): the part above the dotted line in graph (a) is replaced by the part above that line in graph (b). Second, we apply the same rule to replace the part above the upper dotted line in graph (b) by the part above the lower dotted line in graph (c). Keep doing this process until we eliminate all rows of diamonds on the top of the resulting graph. Denote by G'' the final graph (see Figure 3.3(d)).

By removing vertical forced edges at the bottom of G'', we get a the dual graph $\widetilde{G}$ of a weighted semi-hexagon with dents $\mathcal{SH}_{m,n-m}(s_1, \ldots, s_m)$. In particular, the *left rhombi* on the level k (the bottom is at the level 0) are weighted by aq^{k+1}, all *right rhombi* are weighted by b, and all *vertical rhombi* have weight 1 (see Figure 3.2 for three types of rhombi). By Lemma 2.4, we obtain

$$\mathrm{M}\left(AR_{m,n}\left(\mathrm{wt}_{c,d}^{a,b}(q)\right)\right) = q^{\frac{(m-1)m(m+1)}{3}}\left(\prod_{k=1}^{m}\Delta_k^{m-k+1}\right)\mathrm{M}(\widetilde{G}). \tag{3.2}$$

Let T be any lozenge tiling of $\mathcal{SH}_{m,n-m}(s_1, \ldots, s_m)$. Encode T as a family of $n-m$ disjoint rhombi-paths connecting the top and the bottom of the region as in Figures 3.4(a) and (b). This implies that

$$\mathrm{M}(\widetilde{G}) = \sum_{\mathbf{P}=(P_1,\ldots,P_{n-m})}\prod_{i=1}^{n-m}\mathrm{wt}(P_i), \tag{3.3}$$

where the sum is taken over all families of disjoint rhombi-paths $\mathbf{P} = (P_1, P_2, \ldots, P_{n-m})$ connecting the top and the bottom of the region, and where $\mathrm{wt}(P_i)$ is the product of weights of all rhombi in P_i.
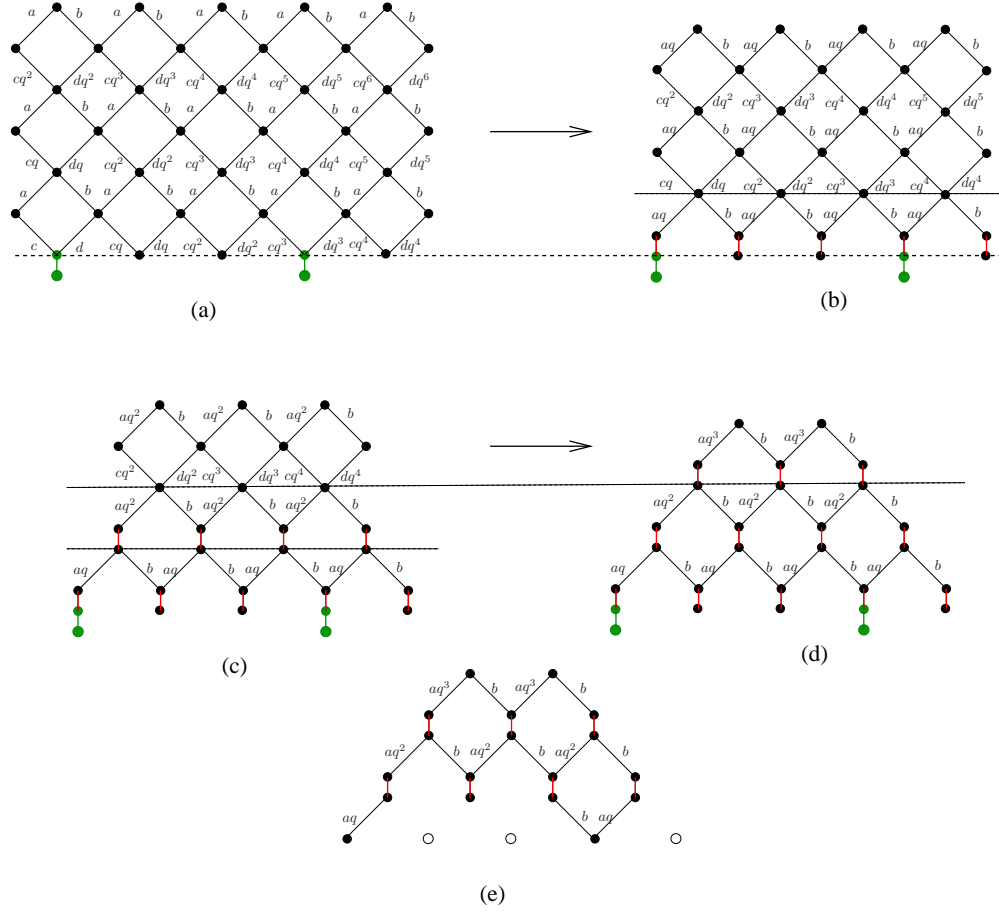
8

Figure 3.3: Transforming an Aztec rectangle graph into the dual graph of a semi-hexagon.

(a)

(b)

(c)

(d)

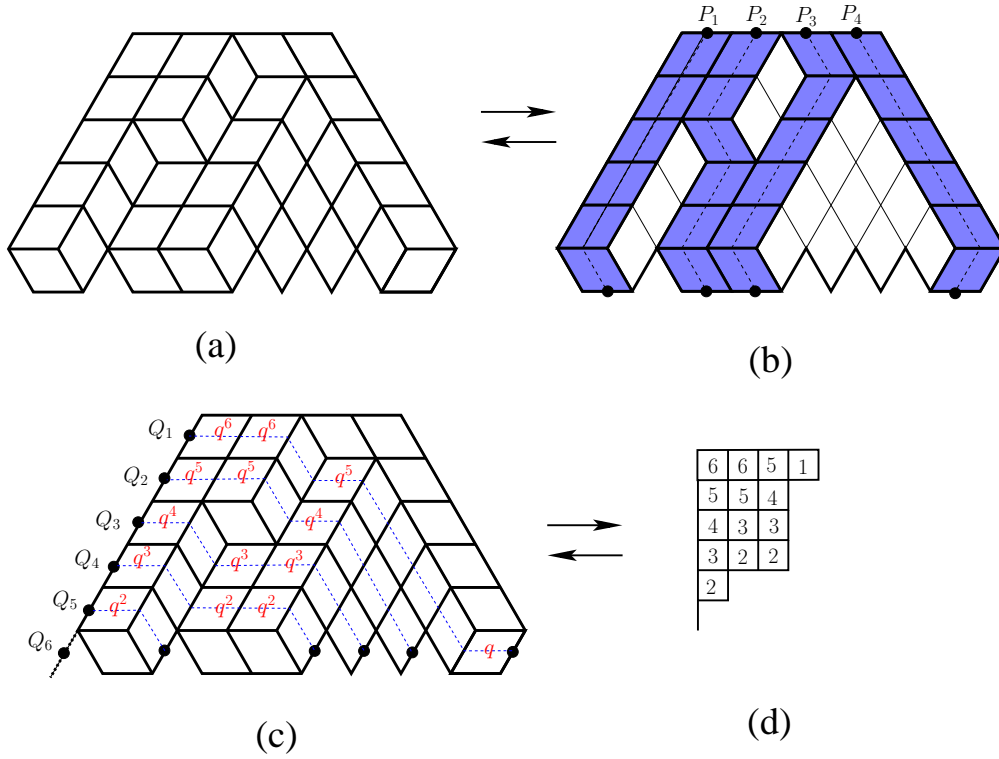Figure 3.4: (a) and (b). Bijection between tilings of a semihexagon $\mathcal{SH}_{6,4}(1,3,6,7,8,10)$ and families of disjoint rhombi-paths. (c) and (d). Bijection between tilings of a semihexagon $\mathcal{SH}_{6,4}(1,3,6,7,8,10)$ and column-strict plane partitions of shape $(10-6,8-5,7-4,6-3,3-2,1-1)$ with positive entries at most 6.

Next, we change the weights of the rhombi as follows. Reassign each right rhombus a weight 1, and divide the weight of each left rhombus by a. Denote by wt' the new weight function. We have $\mathrm{wt}(P_i) = b^{m-s_i+i}a^{s_i-i}\mathrm{wt}'(P_i)$ (since each rhombi-path P_i has exactly $s_i - i$ left rhombi and $m - s_i + i$ right rhombi). Denote by $\overline{G}$ the resulting weighted version of $\widetilde{G}$, and $\overline{\mathcal{SH}}$ the corresponding weighted version of $\mathcal{SH}_{m,n-m}(s_1, \ldots, s_m)$. We get

$$\mathrm{M}(\widetilde{G}) = b^{\sum_{i=1}^{n-m}(m-s_i+i)}a^{\sum_{i=1}^{n-m}(s_i-i)} \sum_{\mathbf{P}=(P_1,\ldots,P_{n-m})} \prod_{i=1}^{n-m} \mathrm{wt}'(P_i)$$

$$= b^{m(n-m)-\sum_{i=1}^{m}(s_i-i)}a^{\sum_{i=1}^{m}(s_i-i)} \mathrm{M}(\overline{G}). \tag{3.4}$$

Now, all left and vertical rhombi in $\overline{\mathcal{SH}}$ are weighted by 1, and each right rhombus on level k is weighted by q^{k+1} (see Figure 3.4(c)).

We now encode each lozenge tiling T of $\overline{\mathcal{SH}}$ as a m-tuple of (new) disjoint rhombi-paths $(Q_1, \ldots, Q_m)$ connecting the northwest side and the left sides of the dents (illustrated in Figure 3.4(c)). Some of the Q_i paths may be empty (when $s_i = i$). The exponents of q along the path Q_i gives the entries of the i-th row of a *column-strict plane partition* of shape $(s_m - m, s_{m-1} - m + 1, \ldots, s_1 - 1)$ with positive entries at most m (see Figure 3.4(d)). We note that path Q_6 in Figure 3.4(c) is empty; and the vertical interval at the bottom of the plane partition in Figure 3.4(d) presents a row of length 0. It is easy to verify that the above correspondence yields a bijection. Moreover, the weight of the tiling T of $\overline{\mathcal{SH}}$ is exactly $q^{|\pi_T|}$, where π_T is the column-strict plane partition corresponding to T and where $|\pi_T|$ is the sum of all entries of π_T.

Summing over all tilings T of $\overline{\mathcal{SH}}$, we have

$$\mathrm{M}(\overline{G}) = \mathrm{M}(\overline{\mathcal{SH}}) = \sum_{\pi} q^{|\pi|} = q^{\sum_{i=1}^{m}(s_i-i)} \prod_{1 \leqslant i < j \leqslant m} \frac{q^{s_j} - q^{s_i}}{q^j - q^i}, \tag{3.5}$$

where the sum after the first equal sign is taken over all column-strict plane partitions π of shape $(s_m - m, s_{m-1} - m + 1, \ldots, s_1 - 1)$ with positive entries at most m; for the second equal sign see e.g. [12], pp. 375. Then the theorem follows from (3.2), (3.4) and (3.5). $\qquad\square$

Remark 1. For $1 \leqslant s_1 < s_2 < \ldots < s_m \leqslant n$, we have the following identity

$$\mathrm{M}(\mathcal{AR}_{m,n}(s_1, s_2, \ldots, s_m)) = 2^{\frac{m(m+1)}{2}} \mathrm{M}(\mathcal{SH}_{m,n-m}(s_1, s_2, \ldots, s_m)), \tag{3.6}$$

where the numbers of tilings on both sides are equal to $2^{\frac{m(m+1)}{2}} \prod_{i<j} \frac{s_j-s_i}{j-i}$ (see e.g. Lemma 3 in [6] and Proposition 2.1 in [3]). This gives an interesting connection between two *different* types of tilings: domino tiling on the left-hand side and lozenge tiling on the right-hand side. By letting $a = b = c = d = q = 1$, Figure 3.3 gives a (simple) combinatorial explanation for the relation (3.6). Moreover, our explanation is direct in the sense that it does not require any explicit enumeration of tilings of the two regions.

4   Proof of Theorem 1.2

A *Schröder path* is a lattice path on $\mathbb{Z}^2$, starting and ending on the x-axis, never going below the x-axis, using $(1, 1)$, $(1, -1)$ and $(2, 0)$ steps (i.e. up, down and level steps, respectively). See Figure 4.1 for a Schröder path.
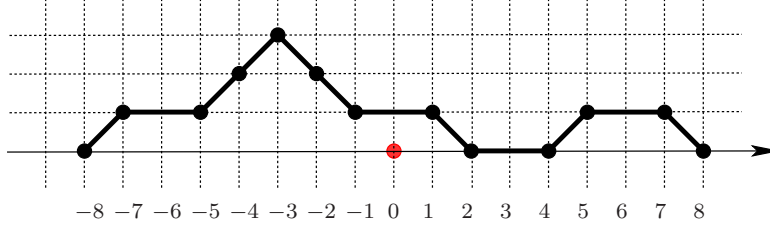
11

Figure 4.1: A Schröder path from $(-8, 0)$ to $(8, 0)$.

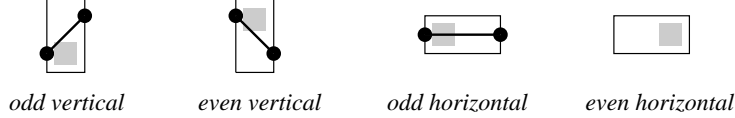*odd vertical*   *even vertical*   *odd horizontal*   *even horizontal*

Figure 4.2: Drawing the steps of the Schröder paths.

Color the Aztec rectangle with holes $\mathcal{AR}_{m,n}(s_1, \ldots, s_m)$ by black and white so that two adjacent unit squares have opposite color and that the unit squares along the northwest side are white. Decorating the dominoes of the region as in Figure 4.2, we have also a bijection between the tilings of the region and families of non-intersecting (partial shifted) Schröder paths $\mathbf{P} = (P_1, P_2, \ldots, P_m)$, where P_i connects the the centers of i-th vertical steps on the southwest and the southeast boundaries of the region (see Figure 4.3).

Assume that the endpoints of P_1 are on the x-axis. Denote by $\text{area}(P_i)$ is the area underneath P_i (i.e. the area restricted by P_i and the x-axis), and define $\text{area}(\mathbf{P}) := \sum_{i=1}^{m} \text{area}(P_i)$. It is easy to see that the family of Schröder paths corresponding to the minimal tiling T_0 has the smallest (total) underneath area (see Figure 4.4).

We assign the dominoes in the Aztec rectangle with holes as follows[1]. Each even horizontal and odd vertical domino a weight 1, each odd horizontal domino on level k from the bottom of the region a weight tq^{2k}, and each even vertical domino on k a weight q^{2k+1} (see Figure 4.2 for four types of dominoes). Similar to the case of rhombi-paths in the previous section, we define the weight $\text{wt}(P_i)$ of the path P_i to be the product of weights of all dominoes corresponding to the steps in P_i; and $\text{wt}(\mathbf{P}) = \prod_{i=1}^{m} \text{wt}(P_i)$. The weight of each tiling of the region can be written as a product of the form $t^x q^y$. Denote by $\beta(\mathbf{P})$ the exponent y of q in the weight $\text{wt}(\mathbf{P}) = \text{wt}(T)$. We denote by $\text{level}(P_i)$, $\text{down}(P_i)$ and $\text{up}(P_i)$ the numbers of level, down and up steps in the path P_i, respectively. Define $\text{level}(\mathbf{P}) := \sum_{i=1}^{m} \text{level}(P_i)$.

Lemma 4.1. *Assume that T is a tiling of the region $\mathcal{AR}_{m,n}(s_1, s_2, \ldots, s_m)$, and $\mathbf{P} = (P_1, P_2, \ldots, P_m)$ is the family of non-intersecting (partial) Schröder paths corresponding to T. Then*

$$v(T) + \text{level}(\mathbf{P}) = \frac{m(m+1)}{2}, \tag{4.1}$$

and

$$\beta(\mathbf{P}) - r(T) = \beta(\mathbf{P}^*) = \sum_{1 \leqslant j \leqslant m} 2(s_i + j - i - 1), \tag{4.2}$$

where $\mathbf{P}^*$ is the path family corresponding to the minimal tiling T_0.

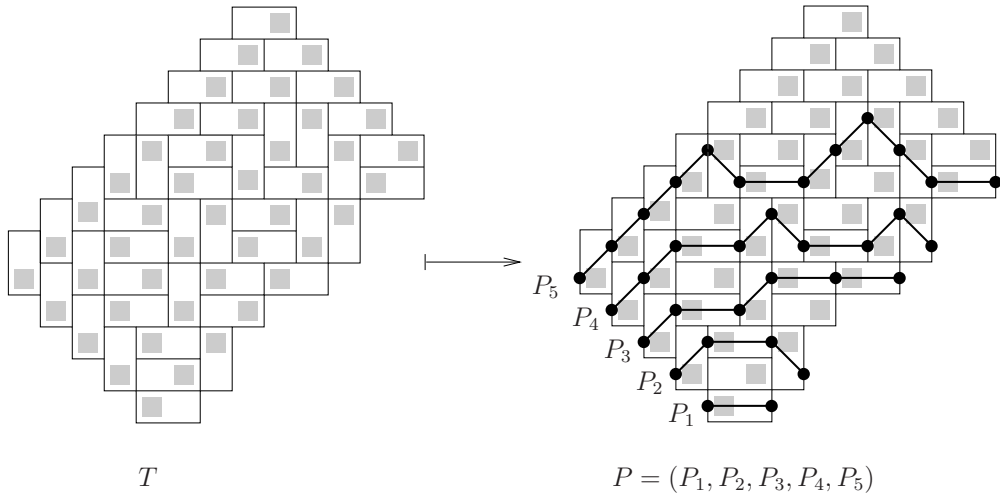[1]This weight assignment was introduced in [7].

T

$P = (P_1, P_2, P_3, P_4, P_5)$

Figure 4.3: Bijection between tilings of an Aztec rectangle with holes and families of non-intersection Schröder paths.

T_0

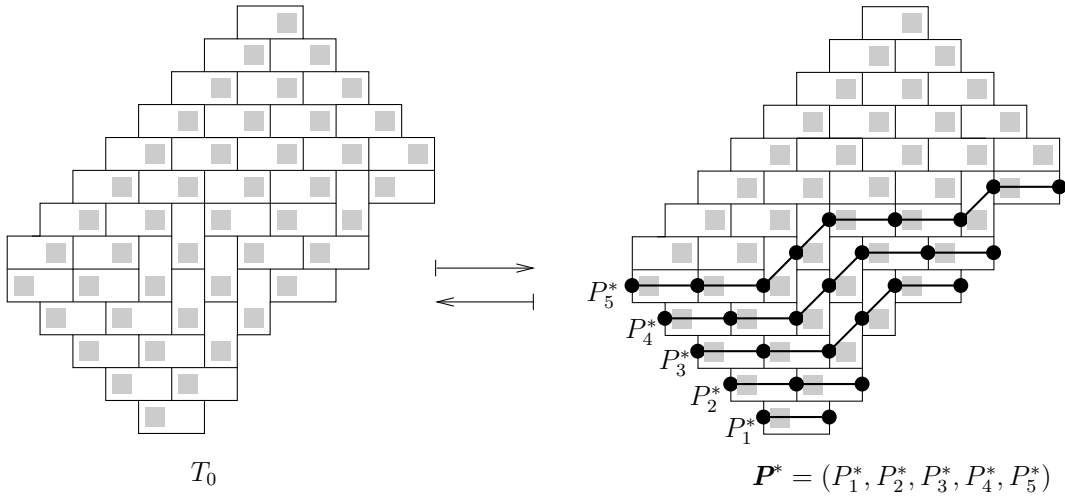$\boldsymbol{P}^* = (P_1^*, P_2^*, P_3^*, P_4^*, P_5^*)$

Figure 4.4: Minimal tiling and its corresponding path family.

Figure 4.5: The elementary moves rise the rank of the tiling T by one (left-to-right, respectively) if only if the exponent of q in $w(T)$ increases by one.

Proof. It is easy to see that

$$\mathrm{up}(P_i) - \mathrm{down}(P_i) = s_i - i. \tag{4.3}$$

Thus, by adding $s_i - i$ down steps to the right of P_i, we have a shifted Schröder path P_i' connecting $(-i, i)$ and $(i + 2(s_i - i), i)$. One readily sees that

$$\mathrm{down}(P_i') = \mathrm{up}(P_i') = \mathrm{up}(P_i), \tag{4.4}$$

$$\mathrm{level}(P_i') = \mathrm{level}(P_i), \tag{4.5}$$

and

$$\mathrm{down}(P_i') = \mathrm{down}(P_i) + (s_i - i). \tag{4.6}$$

Moreover, we have also

$$\mathrm{up}(P_i') + \mathrm{down}(P_i') + 2\,\mathrm{level}(P_i') = 2s_i, \tag{4.7}$$

so by (4.4)

$$\mathrm{down}(P_i') + \mathrm{level}(P_i') = s_i. \tag{4.8}$$

Substituting (4.5) and (4.6) into (4.8), we have

$$\mathrm{down}(P_i) + \mathrm{level}(P_i) = i, \tag{4.9}$$

for any $i = 1, 2, \ldots, m$. Adding m equalities in (4.9), for $i = 1, 2, \ldots, m$, we obtain (4.1).

Divide the set of elementary moves into to types as in Figure 4.5. We notice that the elementary moves (from left to right) increase simultaneously the rank $r(T)$ and the exponent $\beta(\mathbf{P})$ by one. This implies the first equality in (4.2), since $r(T_0) = 0$.

Consider the paths P_j^* in the path family $\mathbf{P}^*$ corresponding to the minimal tiling T_0. The path P_{j+1}^* can be obtained recursively from P_j^* by adding $s_{j+1} - s_j$ up steps followed by a level step, and shifting the resulting path $\sqrt{2}$ units to northwest (see Figure 4.4).

We note that all up steps in P_{j+1}^* have weight 1. Moreover, the above shifting rises simultaneously the weights of all j level steps in P_j^* by a factor q^2; and the weight of the last level step in P_{j+1}^* is $tq^{s_{j+1}-1}$. Thus, we get

$$\mathrm{wt}(P_{j+1}^*) = q^{2j} t q^{2(s_{j+1}-1)} \, \mathrm{wt}(P_j^*), \tag{4.10}$$

and it is easy to see that $\mathrm{wt}(P_1^*) = tq^{2(s_1-1)}$. Thus, by induction, we get

$$\mathrm{wt}(P_j^*) = \prod_{i=1}^{j} t q^{2(s_i + j - i - 1)}, \tag{4.11}$$

for $j = 1, 2, \ldots, m$. Therefore,

$$\mathrm{wt}(T_0) = \mathrm{wt}(\mathbf{P}^*) = t^{\frac{n(n+1)}{2}} q^{\sum_{1 \leqslant i \leqslant j \leqslant m} 2(s_i + j - i - 1)}, \tag{4.12}$$

which implies the second equal sign in (4.2). $\qquad\square$

14

We are now ready to prove Theorem 1.2.

Proof of Theorem 1.2. Weighting the dominoes in our region as in Lemma 4.1. We use the shorthand notation $AR(t,q)$ for the weighted Aztec rectangle graph $AR_{m,n}\left(\text{wt}_{t,q}^{1,1}(q^2)\right)$ in which all bottommost vertices, except for the ones at the positions s_i's, have been removed. Thus, $AR(t,q)$ is simply the dual graph of our weighted region. By the above bijection between domino tilings and families of non-intersecting Schöder paths, we obtain

$$\text{M}(AR(t,q)) = \sum_{\mathbf{P}=(P_1,\ldots,P_m)} \text{wt}(\mathbf{P}) = \sum_{\mathbf{P}=(P_1,\ldots,P_m)} t^{\text{level}(\mathbf{P})} q^{\beta(\mathbf{P})}. \tag{4.13}$$

By Lemma 4.1, we have

$$\sum_T t^{v(T)} q^{r(T)} = q^{-\sum_{1\leqslant i\leqslant j\leqslant m} 2(s_i+j-i-1)} t^{m(m+1)/2} \sum_{\mathbf{P}=(P_1,\ldots,P_m)} t^{-level(\mathbf{P})} q^{\beta(\mathbf{P})} \tag{4.14}$$

$$= q^{-\sum_{1\leqslant i\leqslant j\leqslant m} 2(s_i+j-i-1)} t^{m(m+1)/2} \text{M}(AR(t^{-1},q)), \tag{4.15}$$

and the theorem follows from Theorem 3.1 by letting $a = b = 1$, $c = t^{-1}$, $d = q$, and replacing q by q^2. $\square$

References

[1] F. Bosio and M. A. A. van Leeuwen, *A bijection proving the Aztec diamond theorem by combing lattice paths*, Elec. J. Combin. **20** (4) (2004), P24.

[2] R. Brualdi and S. Kirkland, *Aztec diamonds and digraphs, and Hankel determinants of Schröder numbers*, J. Combin. Theory Ser. B **94** (2) (2005), 334–351.

[3] H. Cohn, M. Larsen and J. Propp, *The Shape of a Typical Boxed Plane Partition*, New York J. of Math. **4** (1998), 137–165.

[4] N. Elkies, G. Kuperberg, M.Larsen, and J. Propp, *Alternating-sign matrices and domino tilings*, J. Algebraic Combin. **1** (1992), 111–132, 219–234.

[5] S.-P. Eu and T.-S. Fu, *A simple proof of the Aztec diamond theorem*, Elec. J. Combin. **12** (2005), R18.

[6] H. Helfgott and I. M. Gessel, *Enumeration of tilings of diamonds and hexagons with defects*, Electron. J. Combin. **6** (1999), R16.

[7] S. Kamioka, *Laurent biorthogonal polynomials, q-Naryana polynomials and domino tilings of the Aztec diamonds*, J. Combin. Theory Ser. A **123** (2014), 14–29.

[8] E. H. Kuo. *Applications of graphical condensation for enumerating matchings and tilings*, Theor. Comput. Sci. **319** (2004), 29–57.

[9] T. Lai, *Enumeration of hybrid domino-lozenge tilings*, J. Combin. Theory Ser. A **122** (2014), 53–81.

[10] T. Lai, *A generalization of Aztec diamond theorem, part I*, Electron. J. Combin. **21**(1) (2014), P1.51.

[11] J. Propp, *Generalized domino-shuffling*, Theor. Comput. Sci. **303** (2003), 267–301.

[12] R. Stanley, *Enumerative Combinatorics*, vol 2, Cambridge Univ. Press., 1999.